

## Radiographic characteristics of the hand and cervical spine in fibrodysplasia ossificans progressiva

Kenichi Mishima<sup>1</sup>, Hiroshi Kitoh<sup>1,2,\*</sup>, Nobuhiko Haga<sup>2</sup>, Yasuharu Nakashima<sup>2</sup>, Junji Kamizono<sup>2</sup>, Takenobu Katagiri<sup>2</sup>, Takafumi Susami<sup>2</sup>, Masaki Matsushita<sup>1</sup>, Naoki Ishiguro<sup>1</sup>

<sup>1</sup> Department of Orthopaedic Surgery, Nagoya University Graduate School of Medicine, Nagoya, Aichi, Japan;

<sup>2</sup> The Research Committee on Fibrodysplasia Ossificans Progressiva, Tokyo, Japan.

### Summary

Fibrodysplasia ossificans progressiva (FOP) is a disabling heritable disorder of connective tissue characterized by progressive heterotopic ossification in various extraskeletal sites. Early correct diagnosis of FOP is important to prevent additional iatrogenic harm or trauma. Congenital malformation of the great toes is a well-known diagnostic clue, but some patients show normal-appearing great toes. The thumb shortening and cervical spine abnormalities are other skeletal features often observed in FOP. This study aimed to address the quantitative assessment of these features in a cohort of patients with FOP, which potentially helps early diagnosis of FOP. Radiographs of the hand and cervical spine were retrospectively analyzed from a total of 18 FOP patients (9 males and 9 females) with an average age of 13.9 years (range 0.7-39.3 years). The elevated ratio of the second metacarpal bone to the distal phalanx of the thumb ( $> +1SD$ ) was a consistent finding irrespective of the patient's age and gender. Infant FOP patients, in addition, exhibited an extremely high ratio of the second metacarpal bone to the first metacarpal bone ( $> +3SD$ ). The height/depth ratio of the C5 vertebra increased in patients over 4 years of age ( $> +2SD$ ). Additionally, the ratio of (height+depth) of the C5 spinous process to the C5 vertebral depth was markedly elevated in young patients ( $> +2SD$ ). We quantitatively demonstrated the hand and cervical spine characteristics of FOP. These findings, which can be seen from early infancy, could be useful for early diagnosis of FOP even in patients without great toe abnormalities.

**Keywords:** Fibrodysplasia ossificans progressiva, early diagnosis, radiographic characteristics

### 1. Introduction

Fibrodysplasia ossificans progressiva (FOP) is a severely disabling genetic disorder of connective tissues characterized by congenital malformations of the great toes and progressive heterotopic ossification (HO) in various extraskeletal sites including muscles, tendons, ligaments, fascias, and aponeuroses. FOP is caused by a recurrent activating mutation (c.617G > A, p.R206H) in the gene encoding activin receptor IA/activin-like kinase 2 (ACVR1/ALK2), a bone morphogenetic protein (BMP) type I receptor (1). HO typically begins

to form during the first decade of life preceded by painful soft tissue swelling and inflammation (flare-ups), which are sometimes mistaken for aggressive fibromatosis or musculoskeletal tumors. Surgical resection of HO leads to explosive new bone formation (2). Since there is no definitive treatment to prevent progressive HO in FOP to date (3), early correct diagnosis is necessary to maintain their mobility by preventing additional iatrogenic harm (4).

Malformations of the great toes, such as hallux valgus, deformed proximal phalanges and shortened first metatarsal bones, are well-known pre-osseous features of FOP (5). A reported incidence of these deformities is 95%, suggesting that there exists rare FOP cases without the great toe abnormalities (6). We demonstrated additional early radiographic signs of FOP including shortening of the first metacarpal bones and hypertrophy of the posterior element of the cervical

\*Address correspondence to:

Dr. Hiroshi Kitoh, Department of Orthopaedic Surgery, Nagoya University Graduate School of Medicine, 65 Tsurumai, Showa-ku, Nagoya, Aichi, 466-8550, Japan.  
E-mail: hkitoh@med.nagoya-u.ac.jp

spine (7). Clinical awareness of these deformities can aid clinicians in making early diagnosis of FOP, but quantitative assessment of these deformities has not yet been determined.

In this study, we retrospectively examined radiographs of the hand and cervical spine in FOP patients and demonstrated various abnormal radiographic parameters helpful for early diagnosis of this specific disorder.

## 2. Materials and Methods

### 2.1. Demographics

This study represents a retrospective case-control study consisting of Japanese FOP patients followed up at health care facilities where members of the Research Committee on Japanese Fibrodysplasia Ossificans Progressiva practiced. After approval from the Institutional Review Board of the Nagoya University Hospital, we collected the hand and/or cervical spine radiographs from 18 FOP patients (9 males and 9 females) with an average age of 13.9 years (range 0.7-39.3 years) at the time of this study. The patients were diagnosed clinically and radiographically based on various characteristic findings of FOP including deformities of the great toes, extraskeletal HO, joint contractures, cervical fusions, broad femoral necks, and osteochondroma-like lesions. Molecular testing was performed on fourteen patients. Thirteen showed the common *ACVR1/ALK2* mutation within the glycine/serine-rich regulatory (GS) domain (c.617G > A, p.R206H), and one patient had an atypical mutation within the protein kinase domain (c.774G > T, p.R258S). Molecular studies were not conducted for the remaining 4 patients who showed characteristic skeletal features of FOP. We examined anteroposterior (AP) radiographs of the hands and lateral radiographs of the cervical spine in each individual. The earliest hands and cervical spine films were analyzed using image processing and analysis software ImageJ®.

### 2.2. Radiographic assessment of the hand

According to the measurement method by Poznanski *et al.* (8), the length of each phalanx and metacarpal bone was measured. In brief, the tangent lines were drawn at both ends of each bone, which were perpendicular to the bone axis, and a bone length was defined as the distance between these two lines (Figure 1). We measured a length of the distal (D1) and proximal (P1) phalanges of the thumb as well as that of the first and second metacarpal bones (MET1 and MET2), and calculated the following bone length ratios, MET2/MET1, MET2/P1, MET2/D1, MET1/P1, MET1/D1, and P1/D1. Radiographs of both hands from one patient were separately analyzed to obtain the average value of the measurements. Reference ranges of these

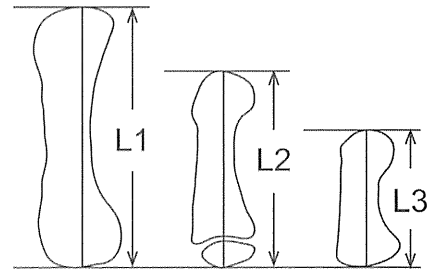


**Figure 1.** A schematic diagram illustrating the measurement method of bone length in the hand. Bone length was defined as the distance between the tangents drawn to each end of the bone, which were perpendicular to the bone axis. The entire bone length was measured for adults (L1), children (L2), and infants (L3).

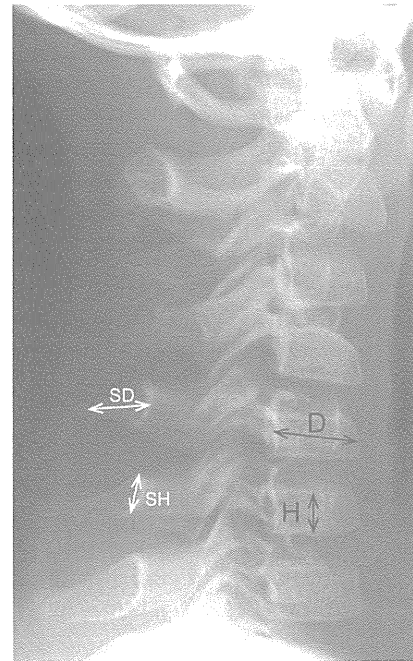


**Figure 2.** A radiograph depicting the measurements of the bone length in the cervical spine. The height (H) and depth (D) of the C5 vertebral body was measured at the midportion of the body. The height of the C5 spinous process (SH) was defined as the distance from the cranial to the caudal rim at the juxta-laminar zone. The depth of the spinous process (SD) was measured from the midpoint of the anterior wall to that of the posterior rim.

measurements in different ages and genders were used based on the literature from Poznanski *et al.* (8). The control data of these measurements in infant ( $n = 21$ ) were determined by the radiographic database in Nagoya University Hospital.

### 2.3. Radiographic assessment of the cervical spine

According to the measurement method proposed by Remes *et al.* (9), the height and depth of the C5 vertebral body were measured. Briefly, vertebral body height (H) was measured at the midpoint of the vertebra, perpendicular to the lower end plate. The vertebral body depth (D) was measured at the midpoint of the body from the anterior wall to the posterior wall (Figure 2). The H/D ratios of the C5 vertebra were then calculated

**Table 1. Characteristics and quantitative indices for the study population**

Patient	Sex	ALK2 mutation	Age at X-ray (yrs)		Deviation of the bone length ratios (SD)			
			Hand/Cervical spine		MET2/D1	MET2/D1	H/D	(SH+SD)/D
1	M	R206H	0/0		1.0	1.0	0.6	0.1
2	M	R206H	0/0		2.4	2.4	0.6	7.1
3	M	R206H	1/3		3.1	3.1	0.9	2.8
4	F	R206H	5/6		2.8	2.8	3.3	8.3
5	M	R206H	8/7		6.2	6.2	2.8	3.7
6	M	R206H	12/18		4.1	4.1	1.9	1.5
7	F	R206H	17/17		4.0	4.0	4.1	NA
8	F	R206H	20/NA		2.2	2.2	NA	NA
9	M	R206H	29/NA		2.7	2.7	NA	NA
10	M	R206H	34/NA		3.5	3.5	NA	NA
11	F	R206H	36/NA		1.0	1.0	NA	NA
12	M	R206H	39/16		1.9	1.9	3.0	1.8
13	F	R206H	NA/18		NA	NA	0.6	2.4
14	F	R258S	14/14		1.7	1.7	4.9	NA
15	M	ND	NA/4		NA	NA	3.2	8.8
16	F	ND	NA/8		NA	NA	9.2	7.9
17	F	ND	NA/16		NA	NA	4.4	NA
18	F	ND	5/5		5.3	5.3	5.3	5.4

M denotes male; F, female; ND, not determined; NA, not applicable; SD, standard deviation.

and compared to normal reference values established by Remes *et al.* in different age and gender groups (9). In addition, we measured the height and depth of the C5 spinous process. The height of the spinous process (SH) was defined as the distance from the cranial to caudal margin at the junction of the spinous process and lamina. The depth of spinous process (SD) was measured from the midportion of the anterior wall to that of the posterior rim demarcating a thick cortex shadow (Figure 2). The sum of SH and SD measurements was used for the evaluation of spinous process size, then the (SH + SD)/D ratio of the C5 vertebra was calculated. Reference values of the (SH + SD)/D ratio were established from the radiographic database of normal controls in Nagoya University Hospital.

### 3. Results

#### 3.1. Characteristics of the study cohort

Patients' characteristics and quantitative indices of the measurements are shown in Table 1. Deviation of the bone length ratios in the hand and cervical spine was calculated based on age-matched reference values.

#### 3.2. Radiographic characteristics of the hand

Mean and standard deviation of the MET2/D1 and MET2/MET1 ratio in control infants ( $n = 21$ ) are  $2.9 \pm 0.29$  and  $1.64 \pm 0.08$ , respectively. Twenty-six hand radiographs from 14 patients (8 males and 6 females) were available. Regardless of age and gender, all FOP patients showed a MET2/D1 ratio larger than +1SD of normal controls (Figure 3A and 3B). In infant patients without an epiphyseal ossification center of the first metacarpal bone, the MET2/MET1 ratio was extremely

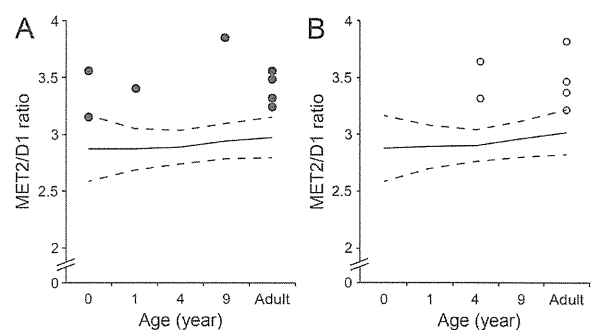


**Figure 3. Scatter plots showing the bone length ratio of the second metacarpal bone (MET2) to the distal phalanx of the thumb (D1) in male (A) and female (B) patients with FOP. Solid and dash lines denote the normal value and the standard deviation (SD) of the MET2/D1 ratio, respectively.**

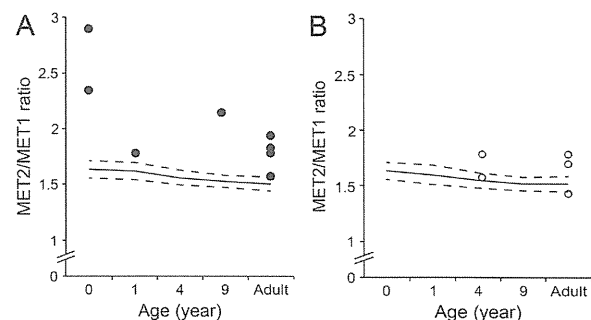


**Figure 4. Scatter plots showing the bone length ratio of the second metacarpal bone (MET2) to the first metacarpal bone (MET1) in male (A) and female (B) patients with FOP. Solid and dash lines denote the normal value and the standard deviation (SD) of the MET2/MET1 ratio, respectively.**

large ( $> +3SD$  of normal controls) (Figure 4A and 4B). The MET2/P1 ratio was higher in infant patients, but it scattered around the mean value with increasing age (data not shown). There were no characteristic features in the values of the MET1/P1, MET1/D1, and P1/D1 ratios in FOP patients, although the MET1/P1 and MET1/D1

**Table 2. Mean and standard deviation of normal controls for the (SH+SD)/D ratio of the C5 vertebra**

Age group	<1	1-2	2-3	3-4	4-5	5-6	6-7	7-8	8-9	9-10	10-11	11-12	12-13	13-14	14-15	15-16	16-17	17-18	18-19	19-20	20-21
Mean	1.05	1.10	1.09	1.20	1.21	1.43	1.37	1.47	1.33	1.47	1.50	1.53	1.51	1.57	1.69	1.86	1.76	1.73	1.71	1.78	1.86
SD	0.13	0.15	0.15	0.13	0.11	0.18	0.18	0.17	0.19	0.18	0.16	0.18	0.20	0.19	0.12	0.16	0.22	0.22	0.23	0.24	0.25
N	11	21	17	13	6	13	25	19	20	17	16	17	14	20	16	21	23	31	28	38	20

SD denotes standard deviation; N, number of control subjects; SH, height of the spinous process; SD, depth of the spinous process; D, depth of the vertebral body.

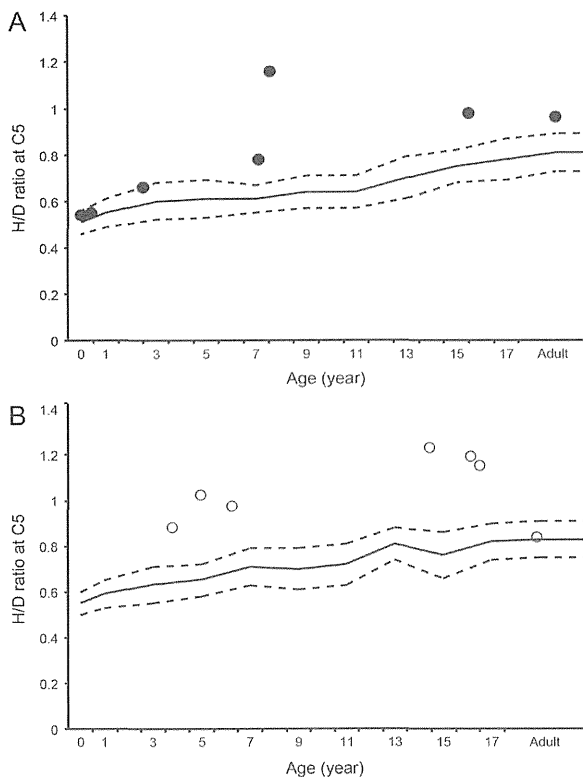


**Figure 5. Scatter plots showing the bone length ratio of the C5 vertebral height (H) to depth (D) in male (A) and female (B) patients with FOP.** Solid and dashed lines denote the normal value and the standard deviation (SD) of the H/D ratio, respectively.

ratios were relatively small ( $< -1SD$  of normal controls) in infant FOP patients (data not shown).

### 3.3. Radiographic characteristics of the cervical spine

Reference values of the (SH + SD)/D ratio of the C5 vertebra are shown in Table 2. There were 14 (7 males and 7 females) cervical spine radiographs available for analysis. Among them, three radiographs were excluded from analysis of the (SH + SD)/D ratio for insufficient resolution. The H/D ratio of the C5 vertebra exceeded +2SD of normal controls in patients over 4 years of age except one female adult patient (Figure 5A and 5B). Similarly, the (SH + SD)/D ratio of the C5 vertebra was larger than +2SD of normal controls in young patients except one male infant (Figure 6).

## 4. Discussion

In the present study, we quantitatively proved the hand

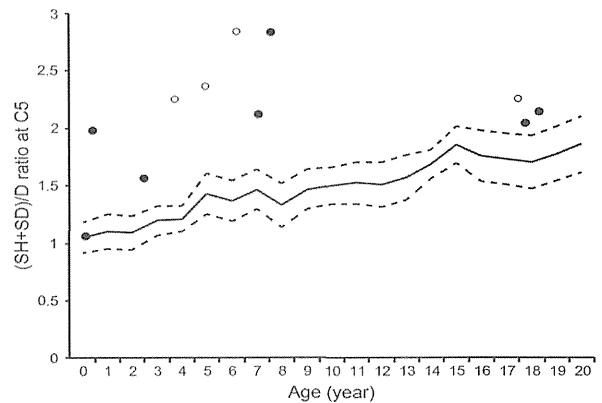


**Figure 6. Scatter plots showing the bone length ratio of the C5 spinous process height (SH) + depth (SD) to the C5 vertebral depth (D).** Solid and open circles indicate male and female, respectively. Solid and dashed lines denote the normal value and the standard deviation (SD) of the (SH+SD)/D ratio, respectively.

and cervical spine abnormalities in FOP including shortened thumbs as well as tall and narrow vertebral bodies and hypertrophic posterior elements of the cervical spine (7,10). Especially in young patients, shortening of the first metacarpal bone and enlargement of the cervical spinous processes were pathognomonic findings useful for early diagnosis of FOP before the appearance of HO.

Previous studies have reported that thumb shortening was seen in 50% of FOP patients (6). In the present study, all patients had a MET2/D1 ratio larger than +1SD of normal controls, and 85% (11/13) of the patients showed an increased MET2/MET1 ratio. The thumb shortening, therefore, seems to be more common than previous reports in FOP. Furthermore, an extremely high MET2/MET1 ratio in infant patients suggested that disproportionate shortening of the first metacarpal bone was an important early radiographic finding in FOP (Figure 7).

It is an intriguing feature of FOP that thumb morphogenesis is exclusively disrupted in the development of digit formation (11). The thumb is the last digit in the autopod to form, and it is different from other digits in terms of its relative position, shape, size, and number of phalanges. These unique thumb identities may be attributed to the expression profile of *HoxD* genes, which are pivotal transcriptional factors regulating limb patterning and growth (12). All four *HoxD10* to *D13* genes are expressed in the future digit II-V area in the autopod during the hand plate formation, whereas sole expression of the

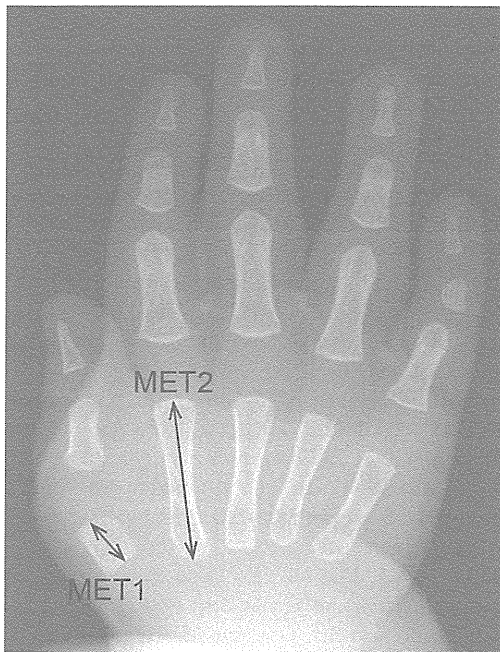


**Figure 7.** An anteroposterior radiograph of the right hand of Patient 1 at the age of eight months showing marked shortening of the first metacarpal bone. The MET2/MET1 ratio and the corresponding SD value is 2.9 and 16.3, respectively.

*HoxD13* gene in the presumptive digit I area is of great significance (13). Mutations in the homeodomain of the *HoxD13* gene cause brachydactyly type D that is characterized by variable shortening of the distal phalanx of the thumb. This mutated *HoxD13* proteins responsible for its decreased affinity for the double-stranded DNA target containing a cognitive sequence of the homeodomain (14). Interestingly, previous research has revealed that BMP signaling-dependent Smad1/4 proteins prevented *HoxD10* and *HoxD13* from binding to DNA targets (15). Constitutively-activated BMP signaling in FOP thus is likely to impair *HoxD13*-mediated transcriptional regulation by direct interactions between BMP-induced Smads and *HoxD13*. Mesenchymal condensation and chondrocyte proliferation of the presumptive digit I area could be suppressed by down-regulated *HoxD13* function, whereas in presumptive digits II to V areas, it could be preserved by compensating expressions of other *HoxD* genes (*HoxD11* and *HoxD12*). Dysregulated BMP signal transduction during embryogenesis seems to cause relative shortening of the first metacarpals and distal phalanges of the thumb in FOP.

More than 90% of adult FOP patients showed fusion of the facet joints, which is a type of orthotopic ossification (6). To our knowledge, however, there are no reports delineating the precise prevalence of tall and narrow vertebral bodies and enlarged posterior elements of the cervical vertebrae. Here we demonstrated that the H/D and (SH + SD)/D ratios in the C5 vertebrae were larger than +2SD of normal values in 64% and 73% of patients, respectively (Figure 8). In addition to

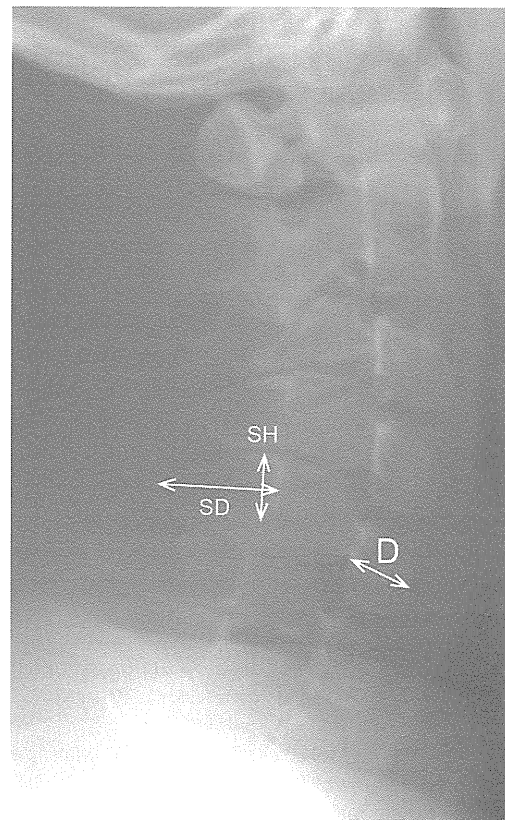


**Figure 8.** A lateral radiograph of the cervical spine of Patient 16 at the age of eight years showing enlarged spinous process of the C5 vertebra. The (SH+SD)/D ratio and the corresponding SD value is 2.8 and 7.9, respectively.

neck stiffness, which seemed to be an important early clinical sign before the appearance of HO (6), tall and narrow vertebrae and hypertrophic spinous processes of the cervical spine are radiographic characteristics in young FOP patients.

In a previous *in vivo* study, genetically-engineered overexpression of BMP-2/4 both dorsally and laterally to the neural tube manifested combined phenotypes of hypertrophic spinous processes and large deletion of the lateral and ventral parts of vertebral bodies (16). Thus, mesenchymal condensations at the paraxial mesoderm in FOP, where BMP-2 signaling is aberrantly activating, could be responsible for both enlarged spinous processes and relatively tall vertebral bodies.

The common *ACVRI/ALK2* mutation (c.617G > A, p.R206H) shows a homogeneous phenotype including congenital malformation of the great toes and the skeletal features in the thumb and cervical spine (17). In contrast, several atypical mutations in the *ALK2/ACVRI* gene, such as L196P, R258S, R375P, G328R, and P197\_F198 del insL, have been identified in patients who showed normal-appearing great toes (18). In this study, one patient (Patient 14) with an atypical mutation (c.774G > C, p.R258S) showed normal-appearing great toes. She also lacked the shortened thumb but exhibited exceptionally tall and narrow vertebral bodies. Another patient (Patient 4) who showed neither malformed great

toes nor shortening of the first metacarpal bone also manifested distinctive features of the cervical spine in spite of the common *ACVR1/ALK2* mutation. We believe that radiographic characteristics of the cervical spine are potent diagnostic clues for FOP especially in cases without typical deformities of the great toes.

### Acknowledgements

This work was supported partly by Research Committee on Fibrodysplasia Ossificans Progressiva from the Ministry of Health, Labour and Welfare of Japan.

### References

1. Shore EM, Xu M, Feldman GJ, *et al.* A recurrent mutation in the BMP type I receptor *ACVR1* causes inherited and sporadic fibrodysplasia ossificans progressiva. *Nat Genet.* 2006; 38:525-527.
2. Kitterman JA, Kantanic S, Rocke DM, Kaplan FS. Iatrogenic harm caused by diagnostic errors in fibrodysplasia ossificans progressiva. *Pediatrics.* 2005; 116:e654-e661.
3. Kitoh H, Achiwa M, Kaneko H, Mishima K, Matsushita M, Kadono I, Horowitz JD, Sallustio BC, Ohno K, Ishiguro N. Perhexiline maleate in the treatment of fibrodysplasia ossificans progressiva: An open-labeled clinical trial. *Orphanet J Rare Dis.* 2013; 8:163.
4. Pignolo RJ, Shore EM, Kaplan FS. Fibrodysplasia ossificans progressiva: Diagnosis, management, and therapeutic horizons. *Pediatr Endocrinol Rev.* 2013; 10 (Suppl 2):437-448.
5. Nakashima Y, Haga N, Kitoh H, Kamizono J, Tozawa K, Katagiri T, Susami T, Fukushi J, Iwamoto Y. Deformity of the great toe in fibrodysplasia ossificans progressiva. *J Orthop Sci.* 2010; 15:804-809.
6. Kaplan FS, Glaser DL, Shore EM, Deirmengian GK, Gupta R, Delai P, Morhart P, Smith R, Le Merrer M, Rogers JG, Connor JM, Kitterman JA. The phenotype of fibrodysplasia ossificans progressiva. *Clin Rev Bone Miner Metab.* 2005; 3:183-188.
7. Mishima K, Kitoh H, Katagiri T, Kaneko H, Ishiguro N. Early clinical and radiographic characteristics in fibrodysplasia ossificans progressiva: A report of two cases. *J Bone Joint Surg Am.* 2011; 93:e52.
8. Poznanski AK, Garn SM, Holt JF. The thumb in the congenital malformation syndromes. *Radiology.* 1971; 100:115-129.
9. Remes VM, Heinenen MT, Kinnunen JS, Martinen EJ. Reference values for radiological evaluation of cervical vertebral body shape and spinal canal. *Pediatr Radiol.* 2000; 30:190-195.
10. Kaplan FS, Le Merrer M, Glaser DL, Pignolo RJ, Goldsby RE, Kitterman JA, Groppe J, Shore EM. Fibrodysplasia ossificans progressiva. *Best Pract Res Clin Rheumatol.* 2008; 22:191-205.
11. Pignolo RJ, Shore EM, Kaplan FS. Fibrodysplasia ossificans progressiva: Clinical and genetic aspects. *Orphanet J Rare Dis.* 2011; 6:80.
12. Oberg KC. Review of the molecular development of the thumb: Digit primera. *Clin Orthop Relat Res.* 2014; 472:1101-1105.
13. Deschamps J. Tailored *Hox* gene transcription and the making of the thumb. *Genes Dev.* 2008; 22:293-296.
14. Johnson D, Kan SH, Oldridge M, Trembath RC, Roche P, Esnouf RM, Giele H, Wilkie AO. Missense mutations in the homeodomain of *HOXD13* are associated with brachydactyly types D and E. *Am J Hum Genet.* 2003; 72:984-997.
15. Li X, Nie S, Chang C, Qiu T, Cao X. Smads oppose *Hox* transcriptional activities. *Exp Cell Res.* 2006; 312:854-864.
16. Monsoro-Burq AH, Duprez D, Watanabe Y, Bontoux M, Vincent C, Brickell P, Le Douarin N. The role of bone morphogenetic proteins in vertebral development. *Development.* 1996; 122:3607-3616.
17. Kaplan FS, Xu M, Glaser DL, Collins F, Connor M, Kitterman J, Sillence D, Zackai E, Ravitsky V, Zasloff M, Ganguly A, Shore EM. Early diagnosis of fibrodysplasia ossificans progressiva. *Pediatrics.* 2008; 121:e1295-e1300.
18. Kaplan FS, Xu M, Seemann P, *et al.* Classic and atypical fibrodysplasia ossificans progressiva (FOP) phenotypes are caused by mutations in the bone morphogenetic protein (BMP) type I receptor *ACVR1*. *Hum Mutat.* 2009; 30:379-390.

(Received April 13, 2014; Revised April 24, 2014; Accepted May 07, 2014)



## ■ CHILDREN'S ORTHOPAEDICS

# Early and late fracture following extensive limb lengthening in patients with achondroplasia and hypochondroplasia

H. Kitoh,  
K. Mishima,  
M. Matsushita,  
Y. Nishida,  
N. Ishiguro

From Nagoya  
University Graduate  
School of Medicine,  
Nagoya, Japan

Two types of fracture, early and late, have been reported following limb lengthening in patients with achondroplasia (ACH) and hypochondroplasia (HCH).

We reviewed 25 patients with these conditions who underwent 72 segmental limb lengthening procedures involving the femur and/or tibia, between 2003 and 2011. Gender, age at surgery, lengthened segment, body mass index, the shape of the callus, the amount and percentage of lengthening and the healing index were evaluated to determine predictive factors for the occurrence of early (within three weeks after removal of the fixation pins) and late fracture (> three weeks after removal of the pins). The Mann-Whitney U test and Pearson's chi-squared test for univariate analysis and stepwise regression model for multivariate analysis were used to identify the predictive factor for each fracture. Only one patient (two tibiae) was excluded from the analysis due to excessively slow formation of the regenerate, which required supplementary measures. A total of 24 patients with 70 limbs were included in the study.

There were 11 early fractures in eight patients. The shape of the callus (lateral or central callus) was the only statistical variable related to the occurrence of early fracture in univariate and multivariate analyses. Late fracture was observed in six limbs and the mean time between removal of the fixation pins and fracture was 18.3 weeks (3.3 to 38.4). Lengthening of the tibia, larger healing index, and lateral or central callus were related to the occurrence of a late fracture in univariate analysis. A multivariate analysis demonstrated that the shape of the callus was the strongest predictor for late fracture (odds ratio: 19.3, 95% confidence interval: 2.91 to 128). Lateral or central callus had a significantly larger risk of fracture than fusiform, cylindrical, or concave callus.

Radiological monitoring of the shape of the callus during distraction is important to prevent early and late fracture of lengthened limbs in patients with ACH or HCH. In patients with thin callus formation, some measures to stimulate bone formation should be considered as early as possible.

**Cite this article: *Bone Joint J* 2014;96-B:1269–73.**

■ H. Kitoh, MD, Associate Professor  
■ K. Mishima, MD, Assistant Professor  
■ M. Matsushita, MD, Assistant Professor  
■ Y. Nishida, MD, Professor  
■ N. Ishiguro, MD, Chair  
Department of Orthopaedic Surgery, Nagoya University Graduate School of Medicine, 65 Tsurumai, Showa ku, Nagoya, Aichi 466 8550, Japan.

Correspondence should be sent to Dr H. K. Kitoh; e-mail: hkitoh@med.nagoya-u.ac.jp

©2014 The British Editorial Society of Bone & Joint Surgery  
doi:10.1302/0301-620X.96B9.33840 \$2.00

*Bone Joint J*  
2014;96-B:1269–73.  
Received 24 January 2014;  
Accepted after revision 16 June 2014

Achondroplasia (ACH) and hypochondroplasia (HCH) are relatively common skeletal dysplasias with disproportionate rhizomelic shortening of the limbs caused by gain-of-function mutations in the fibroblast growth factor receptor 3 (FGFR3).<sup>1–4</sup> Limb lengthening has been used for some patients with these disorders to improve not only the psychological and emotional state but also the quality of life of the patient.<sup>5,6</sup> However, this treatment remains controversial.<sup>7,8</sup> Increasing the magnitude of lengthening is associated with an increase in complications such as premature physal closure, adjacent joint contractures and fractures.<sup>8–10</sup> A fracture may lead to further surgical intervention and prolonged treatment. Despite careful assessment of healing at the time of removal of the fixation

devices, the incidence of fracture remains high, especially in patients undergoing progressive limb lengthening.<sup>11</sup>

Simpson and Kenwright<sup>11</sup> reviewed 173 patients undergoing limb lengthening and recorded that fractures were either early, occurring within a few weeks of removal of the fixator, or late, occurring with the development of deformity several months after the fixator had been removed. In deciding the timing of removal of the fixator and subsequent management, it is important to determine the factors that predispose to these two types of fracture. In this study, we retrospectively reviewed the results of lower limb lengthening for patients with ACH or HCH and analysed the factors influencing the occurrence of early and late fractures.

**Table I.** Categorical and continuous variables of 70 lengthened segments in 24 patients

Categorical variables*	Number of limbs (patients)
Gender (male/female)	30/40 (11/13)
Disease (ACH/HCH)	62/8 (21/3)
Bone (femur/tibia)	26/44
BMI ( $\leq 25$ / $> 25$ )	43/22 (15/9)
Healing index ( $< 50$ / $\geq 50$ )	62/8
Continuous variables	Mean (standard deviation)
Age at operation years	14.6 (4.0) (8 to 24)
Amount of lengthening cm	9.2 (1.3)
Percentage lengthening	44.7 (13.2)

\*ACH, achondroplasia; HCH, hypochondroplasia; BMI, body mass index

## Patients and Methods

Patients with ACH or HCH who underwent lengthening of the lower limbs, with or without simultaneous correction of deformity, at our hospital between 2003 and 2011 and were followed-up for at least 12 months after removal of the fixation pins were included in this study. The diagnosis was made by the characteristic clinical and radiological features and/or FGFR3 genetic studies. We identified 72 lengthening procedures in 25 patients. One patient (two tibiae) required bone grafting and internal fixation due to extremely poor regenerates. As the healing index of this patient could not be evaluated he was excluded, leaving 70 limbs in 24 patients for evaluation, 21 with ACH and three with HCH.

All patients underwent bilateral tibial lengthening. Two were initially treated elsewhere and their tibial analysis was not included. A total of 13 patients (26 femora) underwent bilateral sequential femoral lengthening. Genu varum of  $> 10^\circ$  was corrected during tibial lengthening in six patients (12 tibiae). Categorical and continuous variables of the patients are presented in Table I.

All lengthening was done with a percutaneous osteotomy and the use of a monolateral external fixator (DynaFix rail deformity system, EBI LP, Parsippany, New Jersey). After an initial delay of seven to 14 days, gradual distraction of 0.5 mm twice daily, with or without gradual correction of the deformity, was commenced. The rate of distraction was adjusted so that it did not impair the continuity of the callus on the radiographs. No post-operative immobilisation was used and weight-bearing was encouraged, as tolerated, with the aid of crutches. Distraction was continued until disturbance of gait due to joint stiffness in the lower limbs had become obvious. After distraction was completed, the device was loosened to allow dynamisation of the regenerate as it matured. The decision to remove the fixator was made as a result of at least three paediatric orthopaedic surgeons' consensus (HK, KM, MM), based on the radiological principles of Fischgrund, Paley and Suter<sup>12</sup> which require three of four continuous cortices to have become  $> 2$  mm thick. Initially the frame was removed, leaving the fixation pins *in situ*. After a further one to two weeks, in the absence of fractures or bending at the regenerate, the pins were also removed. All operations and post-operative management were performed by or under the direct supervision of the senior author (HK).

The fractures were described either as early, occurring either during the period of fixation or within three weeks of the pins being removed, or late, occurring  $>$  three weeks after the pins had been removed. Gender, age at surgery, lengthened segment, body mass index (BMI), the shape of the regenerate callus, the amount and percentage of lengthening, and healing index were evaluated to determine the predictive factor for the occurrence of fractures. The BMI at the time of surgery was documented, and patients were categorised as having normal weight (BMI between 18.5 kg/m<sup>2</sup> and 25 kg/m<sup>2</sup>), or being overweight (BMI  $>$  25 kg/m<sup>2</sup>). The shape of the callus was classified into five groups; fusiform (regenerate wider than the original bone), cylindrical (with the same width as the original bone), concave (narrower than the original bone), lateral (mainly on one side of the distraction gap), and central (a thin pillar), based on the width of the callus at the time of removal of the fixator.<sup>13</sup> The total length gained was determined from radiographs taken before the distraction and immediately after removal of the fixation pins, and adjusted for the effect of magnification. The healing index was calculated by dividing the duration of the external fixation (days) by the extent of lengthening (cm) obtained. The distribution of fractures was noted according to the Simpson and Kenwright classification:<sup>11</sup> type 1: fractures within the regenerate, type 2: fractures of the bone/regenerate interface, type 3: fractures at a distance from the callus in the same bone and type 4: fractures of another segment of bone.

**Statistical analysis.** Continuous variables were compared by the nonparametric Mann-Whitney U test and categorical variables by the Pearson's chi-squared test. Finally, independent multivariate predictors for the occurrence of early or late fractures were identified using logistic regression in which all variables with a p-value of  $<$  0.20 from the univariate analysis were entered into a stepwise model for the selection of the explanatory variables. The likelihood ratio, using the chi-squared test, was used to determine the significance of each predictor or possible two-way interactions among variables. Significant predictors of outcome were analysed by calculating the maximal likelihood odds ratio (OR) with 95% confidence intervals (CI). A p-value of  $<$  0.05 was considered statistically significant. Data analysis was performed using JMP version 9 software (SAS Institute, Cary, North Carolina).



**Table II.** Details of 11 early fractures in eight patients

Case	Gender	Age (yrs)	Bone	Site of fracture	Days after frame removal	Days after screw removal	Callus shape	Length (cm)	Length (%)	Healing index (days/cm)	Treatment
1	M	13	T	Type 2	-	2	Central	10	48.5	23.3	Cast
2	M	20	F	Type 1	1	-	Cylindrical	8.8	39	21.6	Re-fixation
3	M	19	F	Type 1	-	5	Cylindrical	6.5	19.6	24.6	Traction
4	F	17	T	Type 1	-	7	Lateral	9.2	46.3	50.3	Cast
5	F	11	T	Type 1	4	-	Central	9.4	67.1	49.8	Re-fixation
		11	T	Type 2	3	-	Concave	9.3	66.4	35.3	Re-fixation
		13	F	Type 2	-	1	Cylindrical	10	50	27.2	Cast
6	M	15	T	Type 1	3	-	Concave	10	45.5	54	Re-fixation
7	M	10	T	Type 2	-	3	Cylindrical	10	46.3	30.7	Cast
		10	T	Type 2	1	-	Lateral	11	52.6	22.2	Op (irrigation, re-fixation)
8	M	14	T	Type 1	1	-	Lateral	8.5	35.4	53.1	Re-fixation

M, male; F, female; T, tibia; F, femur; Op, operation

**Table III.** Details of six late fractures in six patients

Case	Gender	Age (yrs)	Bone	Site of fracture <sup>11</sup>	Days after screw removal	Callus shape	Length (cm)	Length (%)	Healing index (days/cm)	Treatment
1	M	13	T	Type 1	126	Central	10	48.5	23.3	Cast
2	M	11	T	Type 1	167	Concave	8.8	46.8	31.7	Cast
3	F	13	T	Type 1	23	Cylindrical	12	68.2	22.7	Brace
4	F	17	T	Type 2	89	Lateral	9.2	46.3	50.3	Cast
5	M	15	T	Type 1	269	Lateral	10	45.5	54	Crutches
6	F	15	T	Type 1	92	Lateral	8.5	46.2	56.8	Crutches

M, male; F, female; T, tibia; F, femur

## Results

The mean follow-up was 4.6 years (1.7 to 9), and the mean lengthening was 9.2 cm (6 to 12), which resulted in a mean proportional lengthening of 44.7% (19 to 68) of the original bone length. The mean healing index was 34.7 days/cm (18.2 to 117). A healing index of > 50 days/cm was observed in eight bones (11%).

There were 11 early fractures (three femoral and eight tibial) (16%) in eight patients (Table II). All but one fracture occurred without significant trauma. There were six type 1 fractures and five type 2 fractures. A total of six occurred while the pins were *in situ* and five of these were treated successfully with further fixation using the frame. The other patient sustained an open tibial fracture in a fall and was treated with irrigation and re-application of the frame.

The fractures that appeared while the pins were *in situ* occurred within four days of removal of the frame, and five occurred after removal of the pins. The mean delay between removal of the pins and the fracture was 3.6 days (1 to 7). All were minimally displaced and conservatively treated with traction or a cast.

The shape of the callus was cylindrical in four fractures, concave in two, lateral in three, and central in two. All early fractures healed without loss of the length gained or the development of permanent deformity.

Late fracture was observed in six tibiae (Table III). The mean time between removal of the frame and fracture was 18.3 weeks (3.3 to 38.4). There were five type 1 and one type 2 fractures and three had a healing index of > 50 days/cm.

The shape of the callus was lateral in three and cylindrical, concave and central in one each, respectively. A total of four of the fractures were associated with unexpected excessive loading on the affected limb during daily or sporting activities. All were minimally displaced and successfully treated with a cast or a brace. The remaining two patients had an undisplaced stress fracture within the sclerotic regenerate. Reduction of the stress at the fracture site by walking on crutches lead to union.

The shape of the callus was the only variable associated with the occurrence of early fracture in univariate ( $p = 0.001$ ) and multivariate ( $p = 0.005$ ) analyses (Tables IV and V). The rate of early fracture was six in 60 limbs (10%) in fusiform, cylindrical, or concave shaped callus, and five in ten limbs (50%) in either lateral or central shaped callus. The estimated OR of early fracture was nine times higher in the limbs with the latter pattern of callus than in those in the former group (OR 9.00, 95% CI 2.01 to 40.3). Tibial lengthening, healing index and the shape of the callus were related to the occurrence of late fracture in univariate analysis ( $p = 0.049$ ,  $p = 0.002$  and  $< 0.001$ , respectively). The rate of late fracture was much higher in the bones with a healing index of  $\geq 50$  days/cm (3/8 bones, 38%) than in those with a healing index of  $< 50$  days/cm (3/62 bones, 5%). Multivariate logistic regression analysis demonstrated that the shape of the callus was the strongest predictor for late fracture ( $p = 0.002$ ). A callus with a lateral or central shape had a much higher risk of late fracture than other shapes (OR 19.3, 95% CI 2.91 to 128).

**Table IV.** Univariate predictive factors for early and late fractures. Continuous variables are expressed as the mean with standard deviation (SD)

	Presence of an early fracture (n = 11)	Absence of an early fracture (n = 59)	p-value	Presence of a late fracture (n = 6)	Absence of a late fracture (n = 64)	p-value
Gender (male/female)	7/4	23/36	0.129	3/3	27/37	0.712
Age (yrs)	13.9 (SD 3.5)	14.7 (SD 4.10)	0.55	14.0 (SD 2.1)	14.7 (SD 4.3)	0.817
Bone (femur/tibia)	3/8	23/36	0.461	0/6	26/38	0.049*
BMI (normal/high)	7/4	41/18	0.701	3/3	45/19	0.305
Amount of lengthening (cm)	9.3 (SD 1.2)	9.2 (SD 1.3)	0.554	9.8 (SD 1.3)	9.2 (SD 1.3)	0.448
Amount of lengthening (%)	47.0 (SD 13.3)	44.3 (SD 13.3)	0.429	50.3 (SD 8.9)	44.2 (SD 13.5)	0.24
Healing index (< 50/≥ 50)	8/3	54/5	0.072	3/3	59/5	0.002*
Callus shape (F/Cy/Co/ L/Ce)	0/4/2/3/2	7/29/18/5/0	0.001*	0/1/1/3/1	7/32/19/5/1	< 0.001*

BMI, body mass index; F, fusiform; Cy, cylindrical; Co, concave; L, lateral; Ce, central  
\*statistically significant

**Table V.** Multivariate logistic regression analysis for early and late fractures

Early fracture	p-value	Odds ratio	95% CI
Callus shape (F, Cy, Co vs L, Ce)	0.005	9.00	2.01 to 40.3
CI, confidence interval; F, fusiform; Cy, cylindrical; Co, concave; L, lateral; Ce, central			
Late fracture	p-value	Odds ratio	95% CI
Callus shape (F, Cy, Co vs L, Ce)	0.002	19.3	2.91 to 128
CI, confidence interval; F, fusiform; Cy, cylindrical; Co, concave; L, lateral; Ce, central			



Fig. 1a

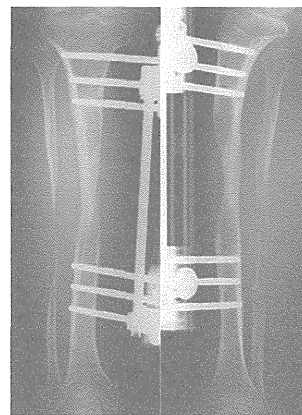


Fig. 1b

Radiographs of the right tibia in a 16-year-old male with achondroplasia with the pins *in-situ* showing a) a minimally displaced tibial fracture (arrow) at the narrowest part of the regenerate. Following minor trauma, this fracture occurred three days after removal of the frame. Figure 2b - the fracture was successfully treated with re-application of the frame for four weeks.

## Discussion

Fracture after extensive limb lengthening in patients with ACH or HCH is still a major complication. Several techniques including CT scan, ultrasound, dual energy X-ray absorptiometry (DEXA), and Orthometry, have been used to evaluate the regenerate and determine when the external fixator should be removed.<sup>14-19</sup> Plain radiographs are, however, usually used to decide when the external fixation should be removed as this is simple and inexpensive. The incidence of early fracture (16%) in our series suggested difficulty in determining the timing of removal of the fixation by radiological appearances alone. Specific criteria for removal of the fixation should be firmly established to prevent fracture of the regenerate.

For fractures which occurred while the pins remained *in situ*, re-application of the frame restored alignment and uneventful healing without additional procedures (Fig. 1). All of these fractures occurred within four days of removal of the frame. Fractures after the subsequent removal of the pins were also observed within a week in all patients. Forriol et al<sup>20</sup> reported in a series studying the radiographs of 55 patients, that fracture occurred in the first two weeks after removal of the fixator in 88% of cases. We thus recommend a period of observation of a few weeks with the pins *in situ* before their final removal.

Bone regenerates are loaded not only in compression but also with bending and torsional stresses after removal of the fixator.<sup>21,22</sup> Since the latter stresses are not encountered during dynamisation, unexpected bending or torsional loads may cause an early fracture. The use of short-term immobilisation by casts or braces after the final removal of the pins could prevent excessive bending or torsional loads.

During a review of 34 lower limb lengthening procedures in patients with ACH and associated conditions, Launay et al<sup>23</sup> reported that the rate of fracture was higher in those aged < nine years. However, we did not find any association between the age of the patient and occurrence of fracture. This may be due to the relative older patients in our series. Simpson and Kenwright<sup>11</sup> reported considerable variation in the location of the 17 fractures that occurred within the regenerate in six, at the bone/regenerate junction in six, and at distant sites in five. In contrast, in our series, most of the early fractures (six, 5%) occurred within the regenerate and there were no fractures at distant sites. Excessive lengthening was occasionally associated with decreased new bone formation in the middle of the regenerate. Venkatesh et al<sup>9</sup> demonstrated that half of the femora in patients with ACH which are lengthened by > 50% of their initial length tended to have a thin or concave shaped callus, some of

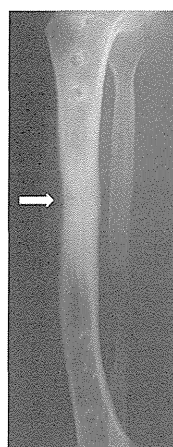


Fig. 2

Lateral radiograph of the right tibia in a 16-year-old female with achondroplasia showing an undisplaced stress fracture of the tibia (arrow) within the hard callus. In the absence of trauma, this fracture was noticed 13.1 weeks after the screws had been removed.

which resulted in fracture. In agreement with their findings, we also observed that most fractures of the regenerate were associated with lateral or central shaped callus. When thin callus is recognised during distraction, attempts should be made to improve the shape of the callus by changing the rhythm of distraction, such as slowing down the rate of distraction, or halting distraction and subsequent compression.<sup>9</sup> Some additional measures to stimulate bone formation should be considered, such as low-intensity pulsed ultrasound or the use of bisphosphonates, osteogenic cytokines or growth factors.<sup>24-27</sup>

There have been few reports describing late fractures after limb lengthening. Faber et al<sup>28</sup> reported seven late fractures in 46 lengthenings, three femoral and four tibial, including one spontaneous fracture in 23 patients. Simpson and Kenwright<sup>11</sup> reported three insidious late fractures with deformities, out of 17 fractures in 180 lengthened segments. These papers, however, lacked a detailed description of the predisposing factors and pattern of late fractures. We clearly demonstrated that bone with a larger healing index and with lateral or central thin callus had a greater risk of late fracture. Delay in consolidation and maturation of the distraction callus leads to prolonged remodelling and insufficient strength of the regenerate. Indeed, in our series, most late fractures occurred in sclerotic regenerates (hard callus) where the medullary cavity was poorly formed (Fig. 2). The excessive loading of vulnerable hard callus should be avoided. For the limbs with thin callus and a larger healing index, careful management will be needed during the formation of the medullary cavity throughout the regenerate, as confirmed on radiographs.

No benefits in any form have been received or will be received from a commercial party related directly or indirectly to the subject of this article.

This article was primary edited by G. Scott and first proof edited by J. Scott.

## References

- Rousseau F, Bonaventure J, Legeai-Mallet L, et al. Mutations in the gene encoding fibroblast growth factor receptor -3 in achondroplasia. *Nature* 1994;371:252-254.
- Shiang R, Thompson LM, Zhu YZ, et al. Mutations in the transmembrane domain of FGFR3 cause the most genetic form of dwarfism, achondroplasia. *Cell* 1994;78:335-342.
- Bellus GA, McIntosh I, Smith EA, et al. A recurrent mutation in the tyrosine kinase domain of fibroblast growth factor receptor 3 causes hypochondroplasia. *Nat Genet* 1995;10:357-359.
- Deng C, Wynshaw-Boris A, Zhou F, Kuo A, Leder P. Fibroblast growth factor receptor 3 is a negative regulator of bone growth. *Cell* 1996;84:911-921.
- Kim SJ, Balce GC, Agashe MV, Song SH, Song HR. Is bilateral lower limb lengthening appropriate for achondroplasia? Midterm analysis of the complications and quality of life. *Clin Orthop Relat Res* 2012;470:616-621.
- Yasui N, Kawabata H, Kojimoto H, et al. Lengthening of the lower limbs in patients with achondroplasia and hypochondroplasia. *Clin Orthop Relat Res* 1997;344:298-306.
- Aldegheri R. Distraction osteogenesis for lengthening of the tibia in patients who have limb-length discrepancy or short stature. *J Bone Joint Surg [Am]* 1999;81-A:624-634.
- Aldegheri R, Dall'Oca C. Limb lengthening in short stature patients. *J Pediatr Orthop B* 2001;10:238-247.
- Venkatesh KP, Modi HN, Devmurari K, et al. Femoral lengthening in achondroplasia: magnitude of lengthening in relation to patterns of callus, stiffness of adjacent joints and fracture. *J Bone Joint Surg [Br]* 2009;91-B:1612-1617.
- Song SH, Kim SE, Agashe MV, et al. Growth disturbance after lengthening of the lower limb and quantitative assessment of physal closure in skeletally immature patients with achondroplasia. *J Bone Joint Surg [Br]* 2012;94-B:556-563.
- Simpson AH, Kenwright SJ. Fracture after distraction osteogenesis. *J Bone Joint Surg [Br]* 2000;82-88.
- Fischgrund J, Paley D, Suter C. Variables affecting time to bone healing during limb lengthening. *Clin Orthop Relat Res* 1994;301:31-37.
- Li R, Saleh M, Yang L, Coulton L. Radiographic classification of osteogenesis during bone distraction. *J Orthop Res* 2006;24:339-347.
- Eyres KS, Bell MJ, Kanis JA. Methods of assessing new bone formation during limb lengthening: ultrasonography, dual energy X-ray absorptiometry and radiography compared. *J Bone Joint Surg [Br]* 1993;75-B:358-364.
- Tselentakis G, Owen PJ, Richardson JB, et al. Fracture stiffness in callotaxis determined by dual-energy X-ray absorptiometry scanning. *J Pediatr Orthop B* 2001;10:248-254.
- Chotel F, Brailon P, Gadeyne S. Bone stiffness in children. Part I. In vivo assessment of the stiffness of femur and tibia in children. *J Pediatr Orthop* 2008;28:534-537.
- Chotel F, Brailon P, Gadeyne S. Bone stiffness in children. Part II. Objective criteria for children to assess healing during leg lengthening. *J Pediatr Orthop* 2008;28:538-543.
- Saran N, Hamdy RC. DEXA as a predictor of fixation removal in distraction osteogenesis. *Clin Orthop Relat Res* 2008;466:2955-2961.
- Song SH, Agashe M, Kim TV, et al. Serial bone mineral density ratio measurement for fixator removal in tibia distraction osteogenesis and need of a supportive method using the pixel value ratio. *J Pediatr Orthop B* 2012;21:137-145.
- Forriol F, Iglesias A, Arias M, Aquerreta D, Cañadell J. Relationship between radiologic morphology of the bone lengthening formation and its complications. *J Pediatr Orthop B* 1999;8:292-298.
- Dwyer JS, Owen PJ, Evans GA, Kuiper JH, Richardson JB. Stiffness measurements to assess healing during leg lengthening: a preliminary report. *J Bone Joint Surg [Br]* 1996;78-B:286-289.
- Windhagen H, Kolbeck S, Bail H, et al. Quantitative assessment of in vitro bone regeneration consolidation in distraction osteogenesis. *J Orthop Res* 2000;18:912-919.
- Launay F, Younsi R, Pithioux M, et al. Fracture following lower limb lengthening in children: a series of 58 patients. *Orthop Traumatol Surg Res* 2013;99:72-79.
- Chan CW, Qin L, Lee KM, et al. Dose-dependent effect of low-intensity pulsed ultrasound on callus formation during rapid distraction osteogenesis. *J Orthop Res* 2006;24:2072-2079.
- Kiely P, Ward K, Bellemore CM, et al. Bisphosphonate rescue in distraction osteogenesis: a case series. *J Pediatr Orthop* 2007;27:467-471.
- Mizumoto Y, Moseley T, Drews M, Cooper VN 3rd, Reddi AH. Acceleration of regenerate ossification during distraction osteogenesis with recombinant human bone morphogenetic protein-7. *J Bone Joint Surg [Am]* 2003;85-A(Suppl3):124-130.
- Kitoh H, Kitakoji T, Tsuchiya H, Katoh M, Ishiguro N. Distraction osteogenesis of the lower extremity in patients with achondroplasia/hypochondroplasia treated with transplantation of culture-expanded bone marrow cells and platelet-rich plasma. *J Pediatr Orthop* 2007;27:629-634.
- Faber FW, Keessen W, van Roermund PM. Complications of leg lengthening: 46 procedures in 28 patients. *Acta Orthop Scand* 1991;62:327-332.

## C-type natriuretic peptide (CNP) plasma levels are elevated in subjects with achondroplasia, hypochondroplasia, and thanatophoric dysplasia

Robert C. Olney,<sup>1</sup> Timothy C.R. Prickett,<sup>2</sup> Eric A. Espiner,<sup>2</sup> William G. Mackenzie,<sup>3</sup> Angela L. Duker,<sup>3</sup> Colleen Ditro,<sup>3</sup> Bernhard Zabel,<sup>4</sup> Tomonobu Hasegawa,<sup>5</sup> Hiroshi Kitoh,<sup>6</sup> Arthur S. Aylsworth,<sup>7</sup> Michael B. Bober<sup>3</sup>

<sup>1</sup>Nemours Children's Clinic, Jacksonville, FL; <sup>2</sup>University of Otago, Christchurch, New Zealand; <sup>3</sup>Nemours/Alfred I. duPont Hospital for Children, Wilmington, DE <sup>4</sup>University Hospital Freiburg, Freiburg, Germany; <sup>5</sup>Keio University School of Medicine, Tokyo, Japan; <sup>6</sup>Nagoya University School of Medicine, Nagoya, Japan; <sup>7</sup>University of N Carolina, Chapel Hill, NC

**Context:** C-type natriuretic peptide (CNP) is a crucial regulator of endochondral bone growth. In a previous report of a child with acromesomelic dysplasia, Maroteaux type (AMDM), due to loss-of-function of the CNP receptor (NPR-B), plasma levels of CNP were elevated. In vitro studies have shown that activation of the MEK/ERK MAP kinase pathway causes functional inhibition of NPR-B. Achondroplasia, hypochondroplasia, and thanatophoric dysplasia are syndromes of short-limbed dwarfism caused by activating mutations of fibroblast growth factor receptor-3, which result in over-activation of the MEK/ERK MAP kinase pathway.

**Objective:** To determine if these syndromes exhibit evidence of CNP resistance as reflected by increases of plasma CNP and its amino terminal propeptide (NTproCNP).

**Design:** This was a prospective, observational study.

**Subjects:** Participants were 63 children and 20 adults with achondroplasia, 6 children with hypochondroplasia, 2 children with thanatophoric dysplasia, and 4 children and 1 adult with AMDM.

**Results:** Plasma levels of CNP and NTproCNP were higher in children with achondroplasia with CNP SD scores (SDS) of 1.0 (0.3–1.4) [median (intraquartile range)] and NTproCNP SDS of 1.4 (0.4–1.8) ( $p < 0.0005$ ). NTproCNP levels correlated with height velocity. Levels were also elevated in adults with achondroplasia, CNP SDS 1.5 (0.7–2.1) and NTproCNP SDS 0.5 (0.1–1.0),  $p < 0.005$ . In children with hypochondroplasia, CNP SDS were 1.3 (0.7–1.5) ( $p = 0.08$ ) and NTproCNP SDS were 1.9 (1.8–2.3) ( $p < 0.05$ ). In children with AMDM, CNP SDS were 1.6 (1.4–3.3) and NTproCNP SDS were 4.2 (2.7–6.2) ( $p < 0.01$ ).

**Conclusions:** In these skeletal dysplasias, elevated plasma levels of proCNP products suggest the presence of tissue resistance to CNP.

C-type natriuretic peptide (CNP) is a member of the natriuretic peptide family that includes atrial natriuretic peptide and B-type natriuretic peptide. The cognate receptor for CNP is natriuretic peptide receptor-B (NPR-B, gene NPR2), a membrane receptor that generates cyclic GMP as the second messenger. C-type natriuretic

peptide is produced in the growth plate and is a potent positive regulator of linear growth (reviewed in 1). Homozygous or biallelic inactivating mutations of NPR2 cause acromesomelic dysplasia, Maroteaux type (MIM 602 875, AMDM), a form of short-limbed dwarfism (2).

C-type natriuretic peptide levels can be measured in

ISSN Print 0021-972X ISSN Online 1945-7197  
Printed in U.S.A.  
Copyright © 2014 by the Endocrine Society  
Received July 1, 2014. Accepted November 6, 2014.

Abbreviations:

plasma, although specific clearance pathways result in low levels. Biosynthetic processing of CNP generates an amino-terminal propeptide (NTproCNP) that is released from the cell in an equimolar ratio to CNP. This propeptide is not subject to specific clearance pathways. As a result, plasma NTproCNP levels reflect CNP production more accurately than levels of the active peptide (3). In a previous report, we documented greatly elevated plasma concentrations of CNP and NTproCNP in a child with AMDM (1), suggesting that reduced intracellular CNP pathway activity may increase CNP production.

Achondroplasia (MIM 100 800) is the most common skeletal dysplasia with incidence estimates ranging from 1 in 15 000 to 1 in 26 000 births (4). Achondroplasia is caused by a mutation in the fibroblast growth factor receptor-3 gene (FGFR3) (5). A single mutation (G380R) accounts for greater than 98% of all reported cases of achondroplasia and is a gain-of-function mutation. Hypochondroplasia (MIM 146 000) is a related, but milder skeletal dysplasia. Thanatophoric dysplasia (MIM 187 600) is a rarer syndrome of skeletal dysplasia, with phenotypic features more severe than in achondroplasia and is often lethal in the neonatal period. Both hypochondroplasia and thanatophoric dysplasia are also caused by gain-of-function mutations in FGFR3 (6, 7).

In the growth plate, FGFR-3 activates a number of signaling cascades, the most important of which appear to be the signal transducers and activators of transcription (STAT1) pathway, which inhibits chondrocyte proliferation, and the MEK/ERK mitogen-activated protein kinase (MAP kinase) pathway, which inhibits chondrocytic differentiation and increases matrix degradation. The net result is poor bone growth (reviewed in 8). The MEK/ERK MAP kinase pathway and the CNP intracellular signaling pathway interact and are mutually inhibitory (9). Evidence of functional inhibition of NPR-B by FGFR-3 overactivity, and our finding of raised plasma CNP peptides in a patient with a homozygous loss-of-function mutation in NPR2, lead us to postulate that plasma levels will also be raised in disorders associated with constitutive activation of FGFR-3.

## Materials and Methods

### Subjects

Subjects were healthy people with the clinical diagnosis of achondroplasia (63 children, 20 adults), hypochondroplasia (6 children), thanatophoric dysplasia (2 children), or AMDM (4 children and 1 adult). This study was approved by the Nemours Florida Institutional Review Board. All children had written parental permission obtained. All adult subjects had written informed consent obtained.

### Study procedures

With the exception of AMDM, this was a prospective study. All subjects with achondroplasia, hypochondroplasia, or thanatophoric dysplasia were seen in the Skeletal Dysplasia Clinic at Nemours/Alfred I. duPont Hospital for Children in Wilmington, DE. Anthropometrics were done, including standing height by wall-mounted tape measure or recumbent length by measuring table and weight by electronic scale. If the subject was an established patient, heights from previous visits were obtained from the medical record for determination of annualized height velocity.

Subjects with AMDM were seen by a variety of geneticists around the world. Blood was drawn locally and plasma was frozen and shipped for analysis.

### Assays

Blood was drawn into EDTA tubes and stored at 4 C until processed. Blood was centrifuged at 4 C and plasma aliquoted and frozen at -80 C until assayed.

The radioimmunoassays used for CNP and NTproCNP were as previously described (10, 11).

### Statistical analysis

Standard deviation scores (SDS) were calculated using the LMS method (12). Height SDS were calculated using Center for Disease Control 2000 data (13). For the subjects with AMDM residing outside the US, country specific height data were used. Standard deviation scores for CNP, NTproCNP, and CNP-to-NTproCNP ratio were calculated using reference data from our previous studies of healthy children (10) and adults (11). Achondroplasia-specific height SDS were calculated using estimates of age-specific mean and SD from height charts reported by Horton, et al (14).

Data are summarized as median and interquartile range (25th - 75th percentiles). For height SDS data, one sample Student's t-tests were used to compare groups to the general population. For the peptide assay data, because of the widely differing ranges of variance in the sample groups, nonparametric tests were used. For the children, comparison between the reference population, and subjects with achondroplasia, hypochondroplasia, or AMDM were made using Kruskal-Wallis tests, with Holm-adjusted Mann-Whitney rank sum tests for post hoc pairwise comparisons. For the adults, comparison of SDS data were made using Mann-Whitney rank sum tests. Correlation between NTproCNP level and height velocity were done by fitting a line by least squares and performing linear regression analysis. Pearson product-moment correlation coefficients ( $r$ ) are reported. Statistics were calculated using Primer of Biostatistics software (version 7; The McGraw-Hill Companies, Inc., New York, NY). Significance was assumed for  $p$  values less than 0.05.

## Results

### Achondroplasia

The characteristics of the subjects with achondroplasia are shown in Table 1. In children with achondroplasia, plasma concentration of both CNP and NTproCNP (Figure 1) were higher than in the reference population ( $P <$

**Table 1.** Subjects with Achondroplasia or Hypochondroplasia

	Achondroplasia		Hypochondroplasia
	children	adults	children
number	63	20	6
sex (F:M)	31:32	11:9	3:3
age (y)	4.7 (2.9–7.5)	41 (36–45)	8.6 (6.6–10.9)
height <i>SD</i> score <sup>a</sup>	−4.8 (−5.6– −4.2)**	ND	−3.1 (−3.7– −2.2)* <sup>†</sup>
height <i>SD</i> score <sup>b</sup>	−0.1 (−0.8–0.5)	ND	1.9 (1.3–3.0) <sup>†</sup>
CNP (pM)	2.1 (1.7–2.4)	0.9 (0.7–1.1)	2.3 (1.9–2.5)
CNP <i>SD</i> score	1.0 (0.3–1.4)**	1.5 (0.7–2.1)*	1.3 (0.7–1.5)*
NTproCNP (pM)	53.0 (47.3–63.0)	17.0 (16.0–19.3)	55.2 (52.1–58.7)
NTproCNP <i>SD</i> score	1.4 (0.4–1.8)**	0.5 (0.1–1.0)*	1.9 (1.8–2.3)*
NTproCNP:CNP ratio	26 (31–22)	21 (16–36)	23 (25–22)
NTproCNP:CNP <i>SD</i> score	−0.1 (−0.7–0.4)	−0.9 (−1.6–0.4)	0.2 (−0.4–0.2)

Data are median (intraquartile range)

ND, not determined

<sup>a</sup>Using general population reference standards

<sup>b</sup>Using achondroplasia-specific reference standards

\* $P < 0.01$  compared to the reference population

\*\* $P < 0.0005$  compared to the reference population

<sup>†</sup> $P < 0.01$ , compared to subjects with achondroplasia

.0005 for both), despite markedly reduced height. Similarly, adults with achondroplasia also had higher levels of CNP and NTproCNP ( $P < .005$  for both)(Table 1). The NTproCNP-to-CNP ratio is a measure of CNP clearance and did not differ from the reference population (Table 1).

Linear regression analysis showed that in children with achondroplasia, NTproCNP level had a significant positive correlation with height velocity ( $n = 62$ ,  $r^2 = 0.42$ ,  $P < .0005$ )(Figure 1, panel C). A similar relationship was found in the reference population ( $n = 139$ ,  $r^2 = 0.51$ ,  $P < .0005$ ) (10). The regression line for children with achondroplasia differed from that of the reference population both for slope ( $1.76 \pm 0.27$  vs.  $2.41 \pm 0.20$  pM/cm/y respectively, mean  $\pm$  SE,  $P < .05$ ) and for intercept ( $46.7 \pm 2.3$  vs.  $24.1 \pm 1.3$  pM,  $P < .0005$ ).

### Hypochondroplasia

Table 1 shows the characteristics of the subjects with hypochondroplasia, all of whom were children. Compared to the reference population, these subjects had elevated plasma CNP and NTproCNP levels (Figure 1)( $P < .05$  for both). Compared to subjects with achondroplasia, the CNP and NTproCNP SDS were not different (Figure 1).

### Thanatophoric dysplasia

We studied two young children with thanatophoric dysplasia. One subject was a 2.3 year old boy with a height SDS of  $-11.5$ . His plasma CNP level was 3.0 pM (SDS of 3.0) and his NTproCNP level was 67.3 (SDS of 1.1). The second subject was a 2.7 year old boy with a height SDS of

$-11.1$ . His plasma CNP level was 1.0 pM (SDS of 0.0) and his NTproCNP level was 72.2 (SDS of 1.8).

### Acromesomelic dysplasia, Maroteaux type

Table 2 shows the characteristics of subjects with AMDM. In the children, CNP SDS ( $n = 3$ ,  $P < .01$ ) and NTproCNP SDS ( $n = 4$ ,  $P < .005$ ) were significantly higher than in the reference population and were also higher than values in achondroplasia (CNP SDS,  $P < .05$ ; NTproCNP SDS,  $P < .005$ , Figure 1). In the adult with AMDM, both plasma CNP and NTproCNP were markedly elevated.

### Discussion

The finding that CNP products in plasma were greatly elevated in a subject with profound short stature due to a disruption of the CNP receptor (NPR-B) and reports from others that activation of the MEK/ERK MAP kinase pathway inhibits NPR-B signaling, lead us to postulate that plasma levels would also be elevated in people with FGFR-3-related skeletal dysplasias such as achondroplasia. The current findings clearly show that circulating products of proCNP are raised not only in children and adults with achondroplasia, but also in children with related conditions of FGFR-3 overactivity.

People with AMDM have absent or disrupted CNP receptors. Since CNP is a growth promoting factor and people with AMDM have profound growth failure, this is a classic instance of hormone resistance. We have shown

**Table 2.** Subjects with Acromesomelic Dysplasia, Maroteaux Type

Age (y)	Genotype	Sex	height SDS	CNP (pM)	CNP SDS	NTproCNP (pM)	NTproCNP SDS	NT:CNP	NT:CNP SDS
2.5	G413E/G413E	M	-5.1	2.7	1.6	86.3	2.8	32.0	-0.5
4.9	del/del	M	-5.3	ND	ND	110.2	5.6		
7.5	R668stop/R218C	F	-2.3	2.1	1.1	58.0	2.4	27.6	-0.6
7.9	I364fs/I364fs	F	-8.5	7.6	5.0	172.0	7.9	22.6	0.1
30	Q853stop/R989 liter	M	-8.6	7.8	46.6	144.0	8.0	18.5	-1.7

ND, not determined

here that CNP and NTproCNP levels are markedly elevated in people with AMDM, suggesting that CNP, as in virtually all other hormone axes, is regulated by a negative feedback loop. Supporting this conclusion are two reports

of subjects with activating mutations of NPR-B causing skeletal overgrowth (15, 16), in whom plasma NTproCNP concentrations were profoundly reduced. Little is known about the factors that regulate CNP expression and translation; the details of this feedback loop require further study.

The interaction between the MEK/ERK MAP kinase and CNP/cGMP pathways has been defined in vitro in chondrogenic cell systems and in organ culture. Phosphorylated MEK1/2 and/or ERK1/2 directly or indirectly inhibit cGMP generation by NPR-B (9). Meanwhile, NPR-B-generated cGMP, in a pathway that involves cGMP-dependent protein kinase II (PRKG2) and the MKK/p38 MAP kinase pathway, inhibits MEK/ERK activation by inhibiting RAF1 (17, 9, 18, 19). Hence in vitro data describe a potential mechanism in which overactivation of the MEK/ERK MAP kinase pathway can result in resistance to CNP.

In this study, we observed a clear increase in CNP and NTproCNP levels in subjects with achondroplasia and hypochondroplasia. We also provide evidence for increased levels in two children with thanatophoric dysplasia, although the sample size was too small for statistical confirmation. Assuming the presence of CNP regulatory feedback loop as suggested by the data from subjects with AMDM, the finding of elevated CNP levels in a population with severe short stature suggests that these individuals may also have resistance to CNP. This is further demonstrated by Figure 1 (panel C), which shows that the slope of the regression line linking NTproCNP and height velocity is significantly reduced in children with achondroplasia compared to the reference population.

There are other potential explanations for our findings. It may be that another branch of the FGFR-3 signaling cascade up-regulates CNP expression and that the MAP kinase inhibition of NPR-B signaling is not occurring or is not relevant in vivo. Another possibility is that the elevated blood levels of CNP are arising from other tissues and not the growth plate and hence not relevant to the growth failure. Now that the observation has been made, further definition is needed to provide clarity. Of interest, products of proCNP in plasma are also elevated in adults with

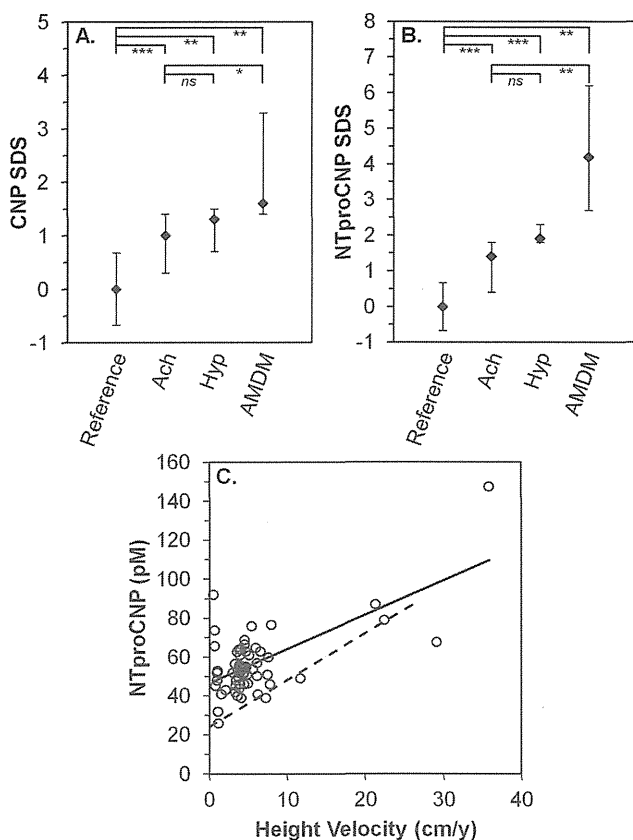


**Figure 1.** C-type natriuretic peptide and NTproCNP levels in children. Panels A & B, comparison between different skeletal dysplasias. Standard deviation scores are shown for CNP (Panel A) and NTproCNP (Panel B) for children from the reference population ( $n = 318$ ), children with achondroplasia ( $n = 63$ , Ach), hypochondroplasia ( $n = 6$ , Hyp), and acromesomelic dysplasia, Maroteaux-type ( $n = 4$ , AMDM). Diamonds show the median for each group and error bars the 25th and 75th percentile. ns, difference is not significant.  $*P < .05$ ;  $**P < .01$ ;  $***P < .0005$ . Panel C shows the correlation between height velocity and NTproCNP levels in children with achondroplasia. Annualized height velocity was determined using the height at a previous clinic visit and the height from the study visit. Solid line, least mean squares linear regression line. The correlation is significant ( $n = 62$ ,  $r^2 = 0.416$ ,  $P < .0005$ ). Dashed line, previously published regression line from children from the general population ( $n = 139$ ,  $r = 0.711$ ,  $P < .0005$ ) (10). The two regression lines differ both in intercept ( $P < .05$ ) and in slope ( $P < .0005$ ).

achondroplasia or AMDM. The tissues that contribute to plasma levels of CNP and NTproCNP after growth plates have closed have not been clearly defined, but are likely to include skeletal, vascular, and cardiac (11, 20) tissue. C-type natriuretic peptide, NPR-B, and FGFR-3 are all expressed in these tissues. The finding of elevated plasma levels of CNP in adults with achondroplasia suggests that alteration of the CNP pathway by activating FGFR3 mutations is not limited to the growth plate.

## Acknowledgments

The authors would like to thank the subjects and their families for participating in this project.

Address all correspondence and requests for reprints to: Robert C. Olney, MD, Nemours Children's Clinic, Jacksonville, FL 32207, (904) 697-3674 fax: (904) 697-3948, rolney@nemours.org.

Disclosure summary: T.C.R.P. and E.A.E. have a patent filed entitled "Assessment of skeletal growth using measurements of NT-CNP peptides"

Clinical Trial Registration Number: NCT01541306

Reprint requests: to corresponding author

This work was supported by Support: developmental funds from Nemours.

## References

1. Olney RC. C-type natriuretic peptide in growth: a new paradigm. *Growth Horm IGF Res.* 2006;16 Suppl A:S6-14.
2. Bartels CF, Bukulmez H, Padayatti P, Rhee DK, Ravenswaaij-Arts C, Pauli RM, Mundlos S, Chitayat D, Shih LY, Al Gazzali LI, Kant S, Cole T, Morton J, Cormier-Daire V, Faivre L, Lees M, Kirk J, Mortier GR, Leroy J, Zabel B, Kim CA, Crow Y, Braverman NE, van den Akker F, Warman ML. Mutations in the Transmembrane Natriuretic Peptide Receptor NPR-B Impair Skeletal Growth and Cause Acromesomelic Dysplasia, *Type Maroteaux*. *Am J Hum Genet.* 2004;75:27-34.
3. Prickett TCR, Espiner EA. 2012 C-type natriuretic peptide (CNP) and postnatal linear growth. 2789-2810.
4. Hunter AG, Bankier A, Rogers JG, Silience D, Scott CI, Jr. Medical complications of achondroplasia: a multicentre patient review. *J Med Genet.* 1998;35:705-712.
5. Shiang R, Thompson LM, Zhu YZ, Church DM, Fielder TJ, Bocian M, Winokur ST, Wasmuth JJ. Mutations in the transmembrane domain of FGFR3 cause the most common genetic form of dwarfism, achondroplasia. *Cell.* 1994;78:335-342.
6. Bellus GA, McIntosh I, Smith EA, Aylsworth AS, Kaitila I, Horton WA, Greenhaw GA, Hecht JT, Francomano CA. A recurrent mutation in the tyrosine kinase domain of fibroblast growth factor receptor 3 causes hypochondroplasia. *Nat Genet.* 1995;10:357-359.
7. Tavormina PL, Shiang R, Thompson LM, Zhu YZ, Wilkin DJ, Lachman RS, Wilcox WR, Rimoin DL, Cohn DH, Wasmuth JJ. Thanatophoric dysplasia (types I and II) caused by distinct mutations in fibroblast growth factor receptor 3. *Nat Genet.* 1995;9:321-328.
8. Foldynova-Trantirkova S, Wilcox WR, Krejci P. Sixteen years and counting: the current understanding of fibroblast growth factor receptor 3 (FGFR3) signaling in skeletal dysplasias. *Hum Mutat.* 2012;33:29-41.
9. Ozasa A, Komatsu Y, Yasoda A, Miura M, Sakuma Y, Nakatsuru Y, Arai H, Itoh N, Nakao K. Complementary antagonistic actions between C-type natriuretic peptide and the MAPK pathway through FGFR-3 in ATDC5 cells. *Bone.* 2005;36:1056-1064.
10. Olney RC, Permuy JW, Prickett TC, Han JC, Espiner EA. Amino-terminal propeptide of C-type natriuretic peptide (NTproCNP) predicts height velocity in healthy children. *Clin Endocrinol (Oxf).* 2012;77:416-422.
11. Prickett TC, Olney RC, Cameron VA, Ellis MJ, Richards AM, Espiner EA. Impact of age, phenotype and cardio-renal function on plasma C-type and B-type natriuretic peptide forms in an adult population. *Clin Endocrinol (Oxf).* 2013;78:783-789.
12. Cole TJ. The LMS method for constructing normalized growth standards. *Eur J Clin Nutr.* 1990;44:45-60.
13. National Center for Health Statistics 2002 2000 CDC Growth Charts for the United States: Methods and Development. *Vital and Health Statistics* 11:1-203.
14. Horton WA, Rotter JL, Rimoin DL, Scott CI, Hall JG. Standard growth curves for achondroplasia. *J Pediatr.* 1978;93:435-438.
15. Miura K, Namba N, Fujiwara M, Ohata Y, Ishida H, Kitaoka T, Kubota T, Hirai H, Higuchi C, Tsumaki N, Yoshikawa H, Sakai N, Michigami T, Ozono K. An Overgrowth Disorder Associated with Excessive Production of cGMP Due to a Gain-of-Function Mutation of the Natriuretic Peptide Receptor 2 Gene. *PLoS One.* 2012;7:e42180.
16. Hannema SE, van Duyvenvoorde HA, Premisler T, Yang RB, Mueller TD, Gassner B, Oberwinkler H, Roelfsema F, Santen GW, Prickett T, Kant SG, Verkerk AJ, Uitterlinden AG, Espiner E, Ruijvenkamp CA, Oostdijk W, Pereira AM, Losekoot M, Kuhn M, Wit JM. An activating mutation in the kinase homology domain of the natriuretic peptide receptor-2 causes extremely tall stature without skeletal deformities. *J Clin Endocrinol Metab.* 2013;98:E1988-E1998.
17. Yasoda A, Komatsu Y, Chusho H, Miyazawa T, Ozasa A, Miura M, Kurihara T, Rogi T, Tanaka S, Suda M, Tamura N, Ogawa Y, Nakao K. Overexpression of CNP in chondrocytes rescues achondroplasia through a MAPK-dependent pathway. *Nat Med.* 2004;10:80-86.
18. Krejci P, Masri B, Fontaine V, Mekikian PB, Weis M, Prats H, Wilcox WR. Interaction of fibroblast growth factor and C-natriuretic peptide signaling in regulation of chondrocyte proliferation and extracellular matrix homeostasis. *J Cell Sci.* 2005;118:5089-5100.
19. Hutchison MR. BDNF alters ERK/p38 MAPK activity ratios to promote differentiation in growth plate chondrocytes. *Mol Endocrinol.* 2012;26:1406-1416.
20. Palmer SC, Prickett TC, Espiner EA, Yandle TG, Richards AM. Regional release and clearance of C-type natriuretic peptides in the human circulation and relation to cardiac function. *Hypertension.* 2009;54:612-618.



